

Electrically Active Domain Wall Magnons in Layered van der Waals Antiferromagnets


Mohammad Mushfiqur Rahman^{1,*}, Avinash Rustagi^{1,‡}, Yaroslav Tserkovnyak², and Pramey Upadhyaya^{1,3,4,†}

¹*Elmore Family School of Electrical and Computer Engineering, Purdue University, West Lafayette, Indiana 47907, USA*

²*Department of Physics and Astronomy, University of California, Los Angeles, California 90095, USA*

³*Purdue Quantum Science and Engineering Institute, Purdue University, West Lafayette, Indiana 47907, USA*

⁴*Quantum Science Center, Oak Ridge, Tennessee 37831, USA*

 (Received 4 May 2022; revised 26 October 2022; accepted 6 December 2022; published 19 January 2023)

We study, theoretically, domain wall (DW) magnons—elementary collective excitations of magnetic DWs—in easy-axis layered van der Waals (vdW) antiferromagnets, where they behave as normal modes of coupled spin superfluids. We uncover that, due to spin-charge coupling in vdW magnets, such DW magnons can be activated by voltage-induced torques, thereby providing a path for their low-dissipation and nanoscale excitation. Moreover, the electrical activation and the number of DW magnons at a frequency can be controlled by applying symmetry-breaking static magnetic field, adding tunability of signal transmission by them. Our results highlight that domain walls in vdW magnets provide a promising platform to route coherent spin information for a broad range of explorations in spintronics and magnetism.

DOI: [10.1103/PhysRevLett.130.036701](https://doi.org/10.1103/PhysRevLett.130.036701)

Introduction.—van der Waals (vdW) magnets have recently emerged as an attractive platform to study magnetism in the atomic two-dimensional (2D) limit [1–9]. They offer access to a variety of magnetic phases which can be controlled by tuning: number of layers [2], stacking order [3,4], Moiré potentials [5,10–12], charge environment [6–8], and proximity effects [9]. This has set the stage to discover magnetic phenomena unique to vdW magnets, along with creating previously unavailable functionalities for spintronics.

A phenomena of central importance in magnetism and spintronics is the coupling of charge degree of freedom with magnons, the (quanta of) elementary collective excitation of magnets [13]. In particular, magnon modes that are attracting significant recent interest are domain wall (DW) magnons—wavelike excitations confined and propagating along topological defects separating differently oriented magnetic regions [14,15]. Such DW magnons provide model systems to explore spin superfluidity [16] and enable imaging of noncollinear phases [17]. Furthermore, owing to nanoscale channeling [15,18], reconfigurability [19,20], and the possibility of transmission along arbitrary-shaped waveguides [15], they offer promising building blocks to wire a broad range of magnon-based classical and quantum circuits [19,21].

So far, coupling the charge degree of freedom with the DW magnons has, however, remained challenging. DW magnons are thus typically excited by the application of oscillating magnetic fields via a microwave antenna [15]. Such an antenna-based driving scheme limits the opportunities for exploiting DW magnons. First, it is difficult to localize the antenna-generated fields at nanoscale [22], which compromises the complexity and scalability of

magnonic circuits that can be built using DW magnon-based nanoscale interconnects. This is because it limits (a) how close two interconnects can be brought without having spurious excitations, and (b) the wavelength of DW magnons that can be excited within each interconnect. Second, the microwave antenna-based excitation is also known to be power hungry [23], which undermines the advantages of low dissipation propagation offered by the DW magnons.

In this Letter, motivated by recent intense interest in layered vdW antiferromagnets (AFMs) [6,8,24–27], we propose and study, theoretically, the electrical excitation of DW magnons in them. Interestingly, we find that the DW magnons in this case behave as the normal modes of coupled DW spin superfluids, which exhibit several unique characteristics when compared to typically studied DW magnons in ferromagnets [15,16,18]. First, there exists two gapless modes, corresponding to stringlike displacement of the DW position and superfluidlike transport of spin current by the DW angle, respectively. Each of these modes disperses linearly as a consequence of the Goldstone theorem, which is similar to DW magnons in conventional antiferromagnets [28]. However, different from the conventional antiferromagnets, where the exchange interaction between sublattice atoms is large and challenging to tune by voltage, the interlayer exchange between 2D layered antiferromagnets is small and readily tunable by voltage [6,8]. We exploit this fact to show that DW magnons in layered vdW antiferromagnets are *electrically active*; oscillating voltage, by coupling directly with the superfluidlike and stringlike mode variables, applies torque on DW magnons and triggers their dynamics. Moreover, exploiting the distinct profile and symmetries of these modes we show

that their electrical activity can be selectively turned on and off via static external magnetic fields. This adds the attractive feature of tunability to the signal transmission by them. Finally, taking advantage of the local nature of the electrical activation, we also demonstrate the excitation of DW magnons with nanoscale wavelengths.

Our Letter extends the scope of unique functionalities offered by vdW magnets to routing of coherent spin signals. Furthermore, it highlights that vdW magnets provide another platform to study coherent spin transport phenomena, such as superfluidlike spin transport, which can be probed electrically via the proposed voltage-induced torques. Such torques, could also be used to electrically probe other exotic dynamic magnetic phenomena in insulating vdW magnets, such as the presence of Moiré magnons [11].

Central scheme.—As a concrete example, we consider an AFM DW hosted within bilayers of an easy-axis layered vdW AFM [Fig. 1(a), with the easy axis oriented along the z axis]. This AFM DW can be viewed as two intralayer ferromagnetic (FM) DWs coupled antiferromagnetically via an interlayer exchange. Such AFM DWs can either be written electrically [8,29] or form naturally [30,31]. To describe the DW magnons in this system, we begin by first focusing on the limit of zero interlayer exchange coupling. In this case, the DW magnons become the dynamical

modes of two decoupled intralayer FM DWs in an easy-axis magnet. For each DW, the spin within the DW region is oriented along an arbitrary angle ϕ in the plane orthogonal to the easy axis, which spontaneously breaks the $U(1)$ symmetry associated with rotations of ϕ in easy-axis magnets. Consequently, the dynamical mode of such DWs coincides with the $U(1)$ symmetry-restoring Goldstone mode. In close analogy with superfluids, this mode transports spin projected along the easy-axis via gradients of ϕ , and is thus referred to as the superfluidlike mode [16]. In FM, the DW position y (here we have defined position normalized to the domain wall width), is canonically coupled with ϕ [16]; the superfluidlike mode thus corresponds to harmonic spatiotemporal variations of the canonically conjugate pair (y, ϕ) .

Turning on a finite interlayer exchange hybridizes the superfluidlike modes living within each layer. The corresponding hybridized normal modes can be described by a new set of canonically conjugate pairs (y_-, ϕ_-) and (y_+, ϕ_+) ; the difference in the two DW positions $y_- \equiv y_1 - y_2$ (proportional to an out-of-plane spin density) acts as a generator of spin rotations in the xy plane, as described by $\phi_+ \equiv \phi_1 + \phi_2$. On the other hand, the canting of DW spins $\phi_- \equiv \phi_1 - \phi_2$ (proportional to an in-plane spin density) induces spin rotations in the xz plane (equivalent to the translation of the AFM DW).

In contrast to the FM case, the position of the AFM DW (y_+), which spontaneously breaks the translation symmetry, becomes decoupled with spin rotations in the xy plane (ϕ_+), which spontaneously breaks the $U(1)$ spin-rotation symmetry. Thus, now there are *two* independent Goldstone modes stemming from *two* continuous symmetries broken by the AFM DW ground state. Consequently, bilayers of layered vdW AFMs support two types of DW magnons—describing harmonic spatiotemporal variations of (y_+, ϕ_-) (stringlike) and (y_-, ϕ_+) (superfluidlike)—with each mode dispersing linearly in the long-wavelength limit [see Figs. 1(c) and 1(d), with mode dispersions (as calculated below) shown in Fig. 1(b)].

Moreover, the interlayer hybridization in vdW magnets can be tuned *dynamically* by voltage, for example via a gate coupled capacitively to it [6,8,24] [Fig. 1(a)]. This novel functionality can activate the superfluidlike and stringlike modes electrically as follows. In the presence of a fixed external magnetic field H applied along the z (y) axis, the competition between Zeeman and interlayer exchange energy creates finite $y_-(\phi_-)$, whose value is controlled by the strength of interlayer exchange for a given H . Electrical modulation of interlayer exchange thus couples $y_-(\phi_-)$ to the voltage for H along z (y). Therefore, an ac voltage with the frequency matched with the DW magnons triggers propagating superfluidlike and/or stringlike modes depending on the orientation of the external magnetic field.

Demonstrating these electrically active modes, by combining analytics with micromagnetic simulations, and

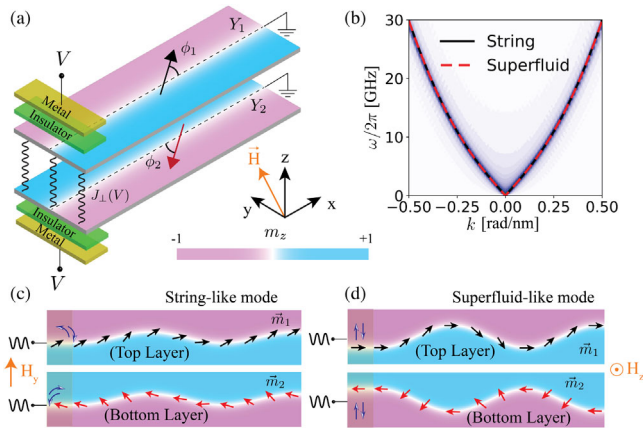


FIG. 1. (a) Schematic of the proposed geometry for the spin wave excitation scheme in the DWs of a bilayer vdW AFM via capacitive coupling to electrical gates. Black and red arrows represent DW spins of the top and bottom layers, parameterized by planar angles $\phi_{1,2}$ and normalized positions $y_{1,2} = Y_{1,2}/\lambda$, where $\lambda = \sqrt{A/K}$ is the DW width. The equilibrium configuration of the DWs are sketched by the dashed straight line. (b) Calculated dispersions using both analytics (solid and dashed lines) and micromagnetic [32] simulations (background) for the string- and superfluidlike modes (see main text for details) in the absence of bias fields. (c),(d) An illustration of the propagating DW magnetization profile for the string- and superfluidlike modes. The double arrows under the gate terminals in (c) and (d) represent, respectively, the oscillations in the orientation of DW spins and the position of the DW due to the application of an oscillating voltage as explained in the central scheme.

highlighting their advantages for routing coherent information are the main focus of the remainder of this Letter.

Model.—We are particularly interested in the low-energy excitations above the equilibrium configuration of an AFM DW oriented, for simplicity, along a straight line (defined as $y = 0$; see Fig. 1). Furthermore, we focus on the low-temperature (compared to the ordering temperature) regime and neglect thermal fluctuations. Within the collective coordinate approach [37,38], the Hamiltonian capturing such dynamics is given by (see Supplemental Material [32] for a detailed derivation)

$$\mathcal{H}_{\text{DW}} = \lambda \int dx \left[\sum_{i=1,2} 2A[(\partial_x y_i)^2 + (\partial_x \phi_i)^2] + J_{\perp}[(y_1 - y_2)^2 + (\phi_1 - \phi_2)^2] \right]. \quad (1)$$

Equation (1) includes contributions from intralayer ferromagnetic exchange (A) and interlayer exchange coupling (J_{\perp}). We note that, due to the last term in Eq. (1), a finite J_{\perp} hybridizes the uncoupled FM DW modes [described by the harmonic variation of (y_i, ϕ_i)]. As highlighted in the central scheme section, this will give rise to new normal modes: superfluidlike (y_{-}, ϕ_{+}) and stringlike (y_{+}, ϕ_{-}), which can be seen explicitly from the equation of motion [see Eq. (2)] as derived next.

In particular, we are interested in determining the dynamics of the AFM DWs in the presence of capacitively coupled gate-voltage drives, external bias magnetic field (in the yz plane), and dissipation. The latter two are added by including Zeeman interaction (\mathcal{H}_z) and Rayleigh function (R), which can be written in terms of the field variables as [32,39] $\mathcal{H}_z = -\lambda M_s \int dx [\pi H_y (\sin \phi_1 - \sin \phi_2) + 2H_z (y_1 - y_2)]$ and $R = -(\alpha M_s \lambda / 2\gamma) \int dx \sum_{i=\{1,2\}} (\dot{y}_i^2 + \dot{\phi}_i^2)$, respectively. Here, H_i is the component of magnetic field along the i th direction, M_s is the saturation magnetization, α is the Gilbert damping parameter, and $\gamma > 0$ is the gyromagnetic ratio. Restricting the strength of magnetic fields to values that cause small deviations from the equilibrium domain wall configuration sketched in Fig. 1(a), we focus on the regime where $H_y \ll K/M_s$ and $H_z \ll J_{\perp}/M_s$.

For electrical driving, motivated by recent demonstrations [6,8,24], we focus on the geometry where the charges on the top and bottom layers are controlled by gates, which for simplicity are connected to the same voltage V [see Fig. (1)]. In this case, as dictated by the structural and time reversal symmetries, the effect of gate voltage drives is captured by adding the spin-charge coupling term [6,8,24,40]: $\mathcal{H}_{me} = \int dx dy \xi V \vec{m}_1 \cdot \vec{m}_2$, where \vec{m}_1 and \vec{m}_2 are the unit vectors oriented along the magnetization in layers 1 and 2, respectively. This term when expressed in terms of DW fields becomes $\mathcal{H}_{me} = \lambda \int dx \xi V [(y_1 - y_2)^2 + (\phi_1 - \phi_2)^2]$, which can be viewed as voltage tunable

interlayer exchange $J_{\perp}(V) = J_{\perp} + \xi V$, where ξ parameterizes the strength of electrical modulation [41].

We next write the equations of motion by utilizing the Poisson bracket relations between the fields [16]: $\{y_i, \phi_i\} = (-1)^i \delta(x - x') / (2M_s / \gamma)$, which stem from the fact that the total spin pointing along the z direction acts as the generator of spin rotation about the same axis within each layer. When expressed in terms of the superfluidlike and stringlike mode variables identified above, the resultant equations can be written in the linear-response limit as [32]

$$(1 + \alpha^2) \delta \dot{q}_{\text{ST/SF}} = M_{\text{ST/SF}} \delta q_{\text{ST/SF}} + \Delta_{\text{ST/SF}}. \quad (2)$$

Here, $\delta q_{\text{ST}} \equiv [\delta \phi_{-}, \delta y_{+}]^T$ and $\delta q_{\text{SF}} \equiv [\delta \phi_{+}, \delta y_{-}]^T$ are the collective coordinates representing small deviations of the stringlike and superfluidlike mode variables from the equilibrium, $\Delta_{\text{ST}} \equiv \delta \omega_J \phi_{-}^{\text{EQ}} [-\alpha, 1]^T$, $\Delta_{\text{SF}} \equiv \delta \omega_J y_{-}^{\text{EQ}} [-1, -\alpha]^T$, and

$$M_{\text{ST}} = \begin{bmatrix} -\alpha(\omega_J + \omega_{H_y} - \omega_A \partial_x^2) & \omega_A \partial_x^2 \\ \omega_J + \omega_{H_y} - \omega_A \partial_x^2 & \alpha \omega_A \partial_x^2 \end{bmatrix}, \\ M_{\text{SF}} = \begin{bmatrix} \alpha(\omega_A \partial_x^2 - \omega_{H_y}) & \omega_A \partial_x^2 - \omega_J \\ \omega_{H_y} - \omega_A \partial_x^2 & \alpha(\omega_A \partial_x^2 - \omega_J) \end{bmatrix}, \quad (3)$$

with $\omega_J \equiv 2\gamma J_{\perp} / M_s$, $\delta \omega_J \equiv 2\gamma \xi V / M_s$, $\omega_A \equiv 2\gamma A / M_s$, and $\omega_{H_y} \equiv \gamma \pi H_y \phi_{-}^{\text{EQ}} / 4$. This equation of motion is one of the central results of this Letter. We highlight that the equations for the stringlike and superfluidlike mode variables are not coupled, which confirms that these represent the normal modes in the presence of interlayer exchange.

Mode dispersion and electrical excitation.—The dispersion relations corresponding to the stringlike and superfluidlike modes, as obtained by assuming harmonic solutions of Eq. (2) in the limit of zero damping and $V = 0$, become

$$\omega_{\text{ST}} = \sqrt{\omega_A k^2 (\omega_A k^2 + \omega_J + \omega_{H_y})}, \\ \omega_{\text{SF}} = \sqrt{(\omega_A k^2 + \omega_J) (\omega_A k^2 + \omega_{H_y})}. \quad (4)$$

In particular, we see that in the absence of external magnetic field and in the long-wavelength limit both modes become linear and degenerate with $\omega_{\text{ST/SF}} \approx k \sqrt{\omega_A \omega_J}$, understood as the Goldstone modes corresponding to the spin translational and rotational symmetries. These are plotted in Fig. 1(b) and corroborated against micromagnetic simulations [32].

The terms proportional to $\delta \omega_J (\xi V)$ in the equations of motion act as *voltage-induced torques*, which can be utilized to electrically excite the DW modes. In line with the physical picture presented in the central scheme section, such voltage-induced torques require nonzero ϕ_{-}^{EQ} and y_{-}^{EQ} in Eq. (2) to activate the dynamics. For a layered

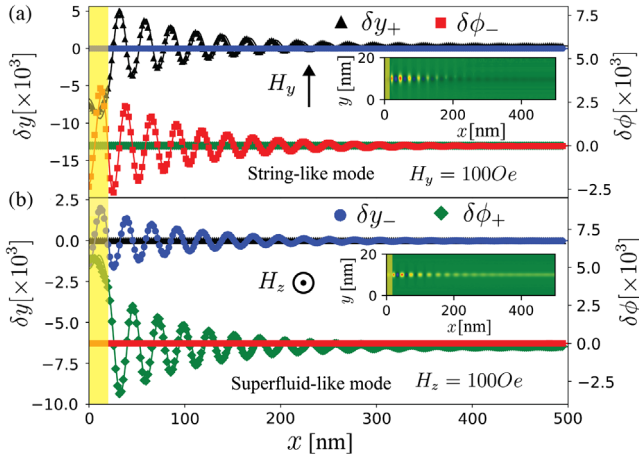


FIG. 2. (a) and (b) Spatial profile of DW mode variables demonstrating their selective excitation via directionally applied fields. Theoretical results (solid) are corroborated against micromagnetic simulations (marker). Insets show micromagnetic simulation snapshots of the propagation of dynamic mode variables. An ac voltage of 4.4 V (equivalent to 10% change in J_{\perp}) was applied to the gates (marked by yellow bars). The parameters for the layered AFM (CrI_3) are $M_S = 1.37 \times 10^{-5}$ emu/cm 2 , $K = 0.26$ erg/cm 2 , $A = 2.29 \times 10^{-15}$ erg, $\alpha = 0.05$, $J_{\perp} = 0.0354$ erg/cm 2 , and $\xi = -8.06 \times 10^{-4}$ ergV $^{-1}$ cm $^{-2}$ [6,8,43].

antiferromagnet, these can be generated by applying H_y and H_z . Therefore, by controlling the direction of external applied static magnetic field a specific mode can be excited electrically.

To confirm this picture, in Figs. 2(a) and 2(b), we plot the dynamic response of DWs as obtained by Eq. (2), as well as, via micromagnetic simulations [42]. As expected, we note that for a y -directed bias field, a stringlike mode (δy_+ , $\delta \phi_-$) is excited, while for the field applied along the z axis, a superfluidlike mode (δy_- , $\delta \phi_+$) is activated. Furthermore, our micromagnetic simulation snapshots (Fig. 2 insets) confirm that the modes are indeed confined within the DW region. The analytic equations of motion exhibit a good quantitative match with our micromagnetic simulations, demonstrating the proposed scheme of electrical driving captures the underlying physics well.

Tunability.—In addition to turning on and off the electrical activity of superfluidlike and stringlike modes, external magnetic field can also tune the group velocity and the number of DW magnons available at a frequency by modifying the mode dispersions. For example, an in-plane field can dramatically tune the properties of a superfluidlike mode. This is because H_y breaks the spin-rotational symmetry and thereby introduces a gap in the superfluidlike mode dispersion. On the other hand, the stringlike mode is left gapless as H_y does not break translation symmetry.

To study such tunability, we show the group velocity of the modes as a function of drive frequency for various values of H_y [Fig. 3(a)], along with the mode dispersions for an exemplary value of $H_y = 500$ Oe [Fig. 3(b)]. We find

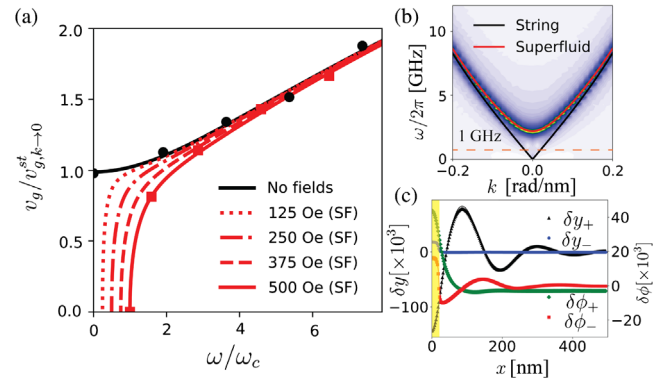


FIG. 3. (a) Analytically calculated (solid lines) and micromagnetic simulations (markers) of group velocity (normalized to $v_{g,k \rightarrow 0}^{\text{ST/SF}} = \sqrt{\omega_A \omega_J}$, the long-wavelength value in the absence of fields) for the string-(blue) and the superfluidlike (red) modes as a function of excitation frequency (normalized to $\omega_c = \sqrt{\omega_J \omega_{H_y}}$, the field-induced gap in superfluidlike mode) for different H_y strengths. (b) Magnon dispersion relations for both modes at $H_y = 500$ Oe. (c) Dynamic response of the DWs obtained via electrically exciting the system at the gapped frequency (1 GHz) demonstrating the excitation of only the stringlike mode variables.

that the superfluidlike mode acquires a gap, which is given by $\omega_c = \sqrt{\omega_J \omega_{H_y}}$, while the stringlike mode remains gapless. Correspondingly, the group velocity of the superfluidlike mode shows tunability over a large range, increasing from zero at $\omega = \omega_c$ and approaching the value for a stringlike mode for large ω . Furthermore, when the applied H_y is such that ω_c is greater than the frequency of the voltage drive, the transmission of the coherent signal is only possible via the stringlike channel. In order to demonstrate this, we apply a canted field with $H_y = H_z$ and excite the system with a frequency below ω_c [Fig. 3(c)]. As both H_y and H_z are nonzero, voltage drives can couple to both stringlike and superfluidlike modes. However, our results clearly demonstrate the excitation of only the stringlike mode.

Nanometer-wavelength excitation.—One outstanding challenge in scaling magnon-based circuits to nanoscale dimensions is the ability to efficiently generate short-wavelength magnons [44–48]. Thanks to the possibility of designing nanoscale gate features, our proposed electrical excitation scheme in vdW magnets provides a route to mitigate this challenge.

To understand the efficiency of voltage-induced excitation and transport at short wavelengths, we study the effect of gate width (L_g) and frequency (equivalently wavelength) on the “spin current” at a particular distance away from the gated region (100 nm from the left edge). To this end, from Eq. (2), considering $\delta \dot{\phi}_- + \alpha \delta \dot{y}_+ - \omega_A (\partial_x^2 \delta y_+) = 0$ and $\delta \dot{y}_- - \alpha \delta \dot{\phi}_+ + \omega_A (\partial_x^2 \delta \phi_+) - \omega_{H_y} \delta \phi_+ = 0$ as the spin continuity relations, the spin currents for the string- and superfluidlike modes are defined as $j_{\text{ST}}(x, t) = -2A \partial_x y_+(x, t)$ and $j_{\text{SF}}(x, t) = 2A \partial_x \phi_+(x, t)$. We plot in

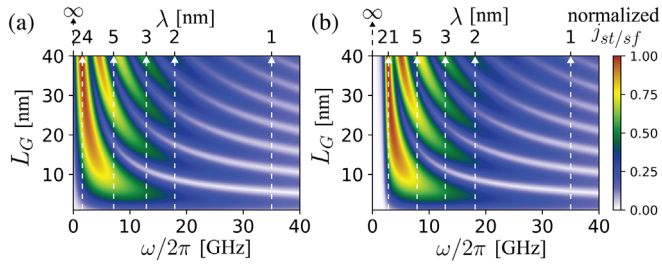


FIG. 4. Analytically calculated spin current amplitudes at a distance $x = 100$ nm from the left edge for the (a) stringlike (j_{ST}) and (b) superfluidlike (j_{SF}) modes as a function of gate width (L_g) and excitation frequency. A canted bias magnetic field with $H_y = H_z = 500$ Oe was applied to excite both the modes.

Fig. 4 the corresponding spin current amplitudes (normalized to the maximum obtained values), which shows an oscillatory dependence on the gate width and frequency before eventually going to zero for high frequency and small gate lengths.

The approach of the spin current to zero can be attributed to the reduction of magnon decay length with higher frequency (due to smaller magnon lifetime $\propto 1/\alpha\omega$) and/or eventual decay of the excitation efficiency. The latter is, in turn, proportional to the Fourier component of the source region at the excitation wavelength [49]. For a rectangular gate, the Fourier component is given by a sinc function of L_g and wavelength, which thus results in the observed oscillatory dependence. Importantly, our results suggest that DW magnons across several wavelengths, reaching as low as few nanometers, can be excited with similar efficiencies by choosing the appropriate gate width.

In summary, we propose domain walls in layered vdW AFMs as promising candidates for nanoscale routing of coherent information. While we have focused on AFM domain walls in easy-axis vdW magnets, the proposed voltage-induced torques can also provide an efficient means to electrically probe noncollinear phases and the flow of low-energy magnons in stacking DWs [11], created, for example, via twisting the vdW bilayers to form a Moiré magnon crystal. Finally, we note that focusing on the low temperature regime and coherent spin dynamics activated by voltage, we have neglected the role of thermal and quantum fluctuations. Addressing their effect on the domain wall ground states and the spin dynamics in layered vdW antiferromagnets could be an interesting future direction.

This work was supported by the National Science Foundation through Grant No. ECCS-1810494.

* rahman62@purdue.edu

† prameyup@purdue.edu

‡ Present address: Intel Corp., Hillsboro, Oregon 97124, USA.

- [1] C. Gong, L. Li, Z. Li, H. Ji, A. Stern, Y. Xia, T. Cao, W. Bao, C. Wang, Y. Wang *et al.*, *Nature (London)* **546**, 265 (2017).
- [2] B. Huang, G. Clark, E. Navarro-Moratalla, D. R. Klein, R. Cheng, K. L. Seyler, D. Zhong, E. Schmidgall, M. A. McGuire, D. H. Cobden *et al.*, *Nature (London)* **546**, 270 (2017).
- [3] N. Sivadas, S. Okamoto, X. Xu, C. J. Fennie, and D. Xiao, *Nano Lett.* **18**, 7658 (2018).
- [4] D. R. Klein, D. MacNeill, Q. Song, D. T. Larson, S. Fang, M. Xu, R. A. Ribeiro, P. C. Canfield, E. Kaxiras, R. Comin *et al.*, *Nat. Phys.* **15**, 1255 (2019).
- [5] Y. Xu, A. Ray, Y.-T. Shao, S. Jiang, D. Weber, J. E. Goldberger, K. Watanabe, T. Taniguchi, D. A. Muller, K. F. Mak *et al.*, *Nat. Nanotechnol.* **17**, 143 (2022).
- [6] S. Jiang, L. Li, Z. Wang, K. F. Mak, and J. Shan, *Nat. Nanotechnol.* **13**, 549 (2018).
- [7] S. Jiang, J. Shan, and K. F. Mak, *Nat. Mater.* **17**, 406 (2018).
- [8] B. Huang, G. Clark, D. R. Klein, D. MacNeill, E. Navarro-Moratalla, K. L. Seyler, N. Wilson, M. A. McGuire, D. H. Cobden, D. Xiao *et al.*, *Nat. Nanotechnol.* **13**, 544 (2018).
- [9] C. Gong and X. Zhang, *Science* **363**, 706 (2019).
- [10] K. Hejazi, Z.-X. Luo, and L. Balents, *Proc. Natl. Acad. Sci. U.S.A.* **117**, 10721 (2020).
- [11] C. Wang, Y. Gao, H. Lv, X. Xu, and D. Xiao, *Phys. Rev. Lett.* **125**, 247201 (2020).
- [12] G. Cheng, M. M. Rahman, A. L. Allcca, A. Rustagi, X. Liu, L. Liu, L. Fu, Y. Zhu, Z. Mao, K. Watanabe *et al.*, *arXiv: 2204.03837*.
- [13] A. Chumak, V. Vasyuchka, A. Serga, and B. Hillebrands, *Nat. Phys.* **11**, 453 (2015).
- [14] J. Winter, *Phys. Rev.* **124**, 452 (1961).
- [15] F. Garcia-Sanchez, P. Borys, R. Soucaille, J.-P. Adam, R. L. Stamps, and J.-V. Kim, *Phys. Rev. Lett.* **114**, 247206 (2015).
- [16] S. K. Kim and Y. Tserkovnyak, *Phys. Rev. Lett.* **119**, 047202 (2017).
- [17] A. Finco, A. Haykal, R. Tanos, F. Fabre, S. Chouaieb, W. Akhtar, I. Robert-Philip, W. Legrand, F. Ajejas, K. Bouzehouane *et al.*, *Nat. Commun.* **12**, 767 (2021).
- [18] Y. Henry, D. Stoeffler, J.-V. Kim, and M. Bailleul, *Phys. Rev. B* **100**, 024416 (2019).
- [19] K. Wagner, A. Kákay, K. Schultheiss, A. Henschke, T. Sebastian, and H. Schultheiss, *Nat. Nanotechnol.* **11**, 432 (2016).
- [20] E. Albisetti, D. Petti, G. Sala, R. Silvani, S. Tacchi, S. Finizio, S. Wintz, A. Calò, X. Zheng, J. Raabe *et al.*, *Commun. Phys.* **1**, 56 (2018).
- [21] J. Lan, W. Yu, R. Wu, J. Xiao, *Phys. Rev. X* **5**, 041049 (2015).
- [22] A. Laucht, J. T. Muhonen, F. A. Mohiyaddin, R. Kalra, J. P. Dehollain, S. Freer, F. E. Hudson, M. Veldhorst, R. Rahman, G. Klimeck, K. M. Itoh, D. N. Jamieson, J. C. McCallum, A. S. Dzurak, and A. Morello, *Sci. Adv.* **1**, e1500022 (2015).
- [23] T. Nozaki, Y. Shiota, S. Miwa, S. Murakami, F. Bonell, S. Ishibashi, H. Kubota, K. Yakushiji, T. Saruya, A. Fukushima *et al.*, *Nat. Phys.* **8**, 491 (2012).
- [24] J. Cenker, B. Huang, N. Suri, P. Thijssen, A. Miller, T. Song, T. Taniguchi, K. Watanabe, M. A. McGuire, D. Xiao *et al.*, *Nat. Phys.* **17**, 20 (2021).

- [25] D. Abdul-Wahab, M. Augustin, S. M. Valero, W. Kuang, S. Jenkins, E. Coronado, I. V. Grigorieva, I. J. Vera-Marun, E. Navarro-Moratalla, R. F. Evans *et al.*, *Adv. Mater.* **33**, 2004138 (2021).
- [26] H. Sun, B. Xia, Z. Chen, Y. Zhang, P. Liu, Q. Yao, H. Tang, Y. Zhao, H. Xu, and Q. Liu, *Phys. Rev. Lett.* **123**, 096401 (2019).
- [27] M. M. Otrokov, I. I. Klimovskikh, H. Bentmann, D. Estyunin, A. Zeugner, Z. S. Aliev, S. Gaß, A. Wolter, A. Koroleva, A. M. Shikin *et al.*, *Nature (London)* **576**, 416 (2019).
- [28] B. Flebus, H. Ochoa, P. Upadhyaya, and Y. Tserkovnyak, *Phys. Rev. B* **98**, 180409(R) (2018).
- [29] T. Song, M. W.-Y. Tu, C. Carnahan, X. Cai, T. Taniguchi, K. Watanabe, M. A. McGuire, D. H. Cobden, D. Xiao, W. Yao *et al.*, *Nano Lett.* **19**, 915 (2019).
- [30] D. Zhong, K. L. Seyler, X. Linpeng, N. P. Wilson, T. Taniguchi, K. Watanabe, M. A. McGuire, K.-M. C. Fu, D. Xiao, W. Yao *et al.*, *Nat. Nanotechnol.* **15**, 187 (2020).
- [31] P. M. Sass, W. Ge, J. Yan, D. Obeysekera, J. Yang, and W. Wu, *Nano Lett.* **20**, 2609 (2020).
- [32] See Supplemental Material at <http://link.aps.org/supplemental/10.1103/PhysRevLett.130.036701> for containing the derivations for the dynamics of the coupled DWs and details of the micromagnetic simulation environment, which includes Refs. [33–36].
- [33] N. L. Schryer and L. R. Walker, *J. Appl. Phys.* **45**, 5406 (1974).
- [34] A. Vansteenkiste, J. Leliaert, M. Dvornik, M. Helsen, F. Garcia-Sanchez, and B. Van Waeyenberge, *AIP Adv.* **4**, 107133 (2014).
- [35] A. G. Gurevich and G. A. Melkov, *Magnetization Oscillations and Waves* (CRC Press, London, 2020).
- [36] G. Venkat, D. Kumar, M. Franchin, O. Dmytriiev, M. Mruczkiewicz, H. Fangohr, A. Barman, M. Krawczyk, and A. Prabhakar, *IEEE Trans. Magn.* **49**, 524 (2012).
- [37] O. A. Tretiakov, D. Clarke, G.-W. Chern, Y. B. Bazaliy, and O. Tchernyshyov, *Phys. Rev. Lett.* **100**, 127204 (2008).
- [38] A. Thiele, *Phys. Rev. Lett.* **30**, 230 (1973).
- [39] G. Tatara, H. Kohno, and J. Shibata, *Phys. Rep.* **468**, 213 (2008).
- [40] A. Rustagi, A. Bharatbhai Solanki, Y. Tserkovnyak, and P. Upadhyaya, *Phys. Rev. B* **102**, 094421 (2020).
- [41] We note that symmetry-allowed spin-charge coupling can generate a variety of terms beyond modulation of interlayer exchange, such as the so-called magnetoelectric term which couples the difference in layer magnetizations to the electric field. Here, since we have focused on the geometry where top and bottom gates are connected to the same voltage, i.e., electric field = 0, such terms are not included. However, our formalism can be trivially generalized to include electric field coupling for future studies.
- [42] These are obtained by directly integrating the Landau-Lifshitz-Gilbert (LLG) equations which is equivalent to applying the Hamilton's equations for the Hamiltonian shown in Eq. (1).
- [43] J. L. Lado and J. Fernández-Rossier, *2D Mater.* **4**, 035002 (2017).
- [44] V. Sluka, T. Schneider, R. A. Gallardo, A. Kákay, M. Weigand, T. Warnatz, R. Mattheis, A. Roldán-Molina, P. Landeros, V. Tiberkevich *et al.*, *Nat. Nanotechnol.* **14**, 328 (2019).
- [45] B. Van de Wiele, S. J. Hämäläinen, P. Baláž, F. Montoncello, and S. Van Dijken, *Sci. Rep.* **6**, 21330 (2016).
- [46] N. J. Whitehead, S. A. R. Horsley, T. G. Philbin, A. N. Kuchko, and V. V. Kruglyak, *Phys. Rev. B* **96**, 064415 (2017).
- [47] B. Mozooni and J. McCord, *Appl. Phys. Lett.* **107**, 042402 (2015).
- [48] C. S. Davies, V. D. Poimanov, and V. V. Kruglyak, *Phys. Rev. B* **96**, 094430 (2017).
- [49] A. Mahmoud, F. Ciubotaru, F. Vanderveken, A. V. Chumak, S. Hamdioui, C. Adelman, and S. Cotofana, *J. Appl. Phys.* **128**, 161101 (2020).